

USNO MASTER CLOCK DESIGN ENHANCEMENTS

P. Koppang, J. Skinner, and D. Johns
U.S. Naval Observatory

Abstract

We have implemented several enhancements to the US Naval Observatory (USNO) Master Clock system. Design changes to the system include the use of a Kalman filter for phase and frequency estimates, decreasing the time interval between steers, and the redesign of control parameters. The present control system utilizes “real-time” data estimates of the differences between the Master Clock and a timescale that combines hydrogen masers and commercial cesium frequency standards with a time-varying weighting scheme. We are researching a Master Clock system design that utilizes as its reference a hydrogen maser ensemble that is steered to an ensemble of cesium standards. We present system designs, simulations, and performance data.

INTRODUCTION

We are implementing and investigating techniques to increase the robustness of the U.S. Naval Observatory (USNO) Master Clock (MC) system while maintaining and/or improving overall performance. There are roughly 60 cesium standards and 20 hydrogen masers contributing to the operational timescale at any given time. These standards are spread throughout several locations and housed in 15 separate environmental chambers at USNO in Washington, DC. Hydrogen masers are approximately an order of magnitude more stable than high-performance commercial cesium standards in the short term, while the cesium standards show better long-term characteristics. Strategies on how to combine these frequency standards to best benefit from their respective strengths are shown along with the evolution of the MC system design. We also discuss the minimal control energy technique and its implementation in steering the MC to UTC as derived by BIPM.

MASTER CLOCK SYSTEM

The USNO MC system consists of atomic frequency standards, signal measurement and distribution components, frequency synthesizers, timescales, and control algorithms. The overall concept of the MC system is to create a physical realization of a robust and stable timescale that represents our best real-time estimate of UTC.

PREVIOUS SYSTEM DESIGN

The previous MC system used dynamic weighting to combine the cesium and hydrogen maser frequency standards into a timescale (also referred to as a mean or ensemble) [1,2]. This timescale weighted masers highly in the recent past with the cesiums receiving a higher weight further into the past. This created a

non-causal timescale that was stable in the short term due to the higher weighted hydrogen masers and gained long-term stability from the cesiums. Clock models were used to mathematically remove best estimates of the characteristic frequency and drift (for masers) from the free-running clock data. In order to create a physical output representing the paper clock timescale, a hydrogen maser was steered to the timescale via a low-noise, high-resolution frequency synthesizer. A block diagram of the system is shown in Figure 1. Steers were made daily based on phase and frequency estimates of the dynamic timescale at the time of the steer. The frequency estimates were particularly sensitive to discrepancies between the cesium and hydrogen maser means.

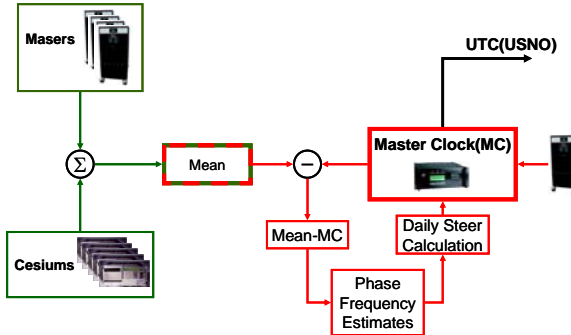


Figure 1. Previous design block diagram.

PRESENT OPERATIONAL SYSTEM DESIGN

The present operational system utilizes the dynamic mean as described in the previous section, but uses a Kalman filter to estimate the phase and frequency offsets between the MC and the mean [3,4]. This gives an optimal real-time estimate that approximates an all hydrogen maser-based mean and solves the frequency bias issue of the previous design. With the goal of increasing robustness, the steering rate was increased from daily to hourly (see Figure 2). The lower-noise estimates and increased data rate allow for a tighter control design that can better react to perturbations that can occur in the reference, or steered, frequency standard. These perturbations may be caused by internal physical changes in the reference standard or external factors such as environmental disturbances.

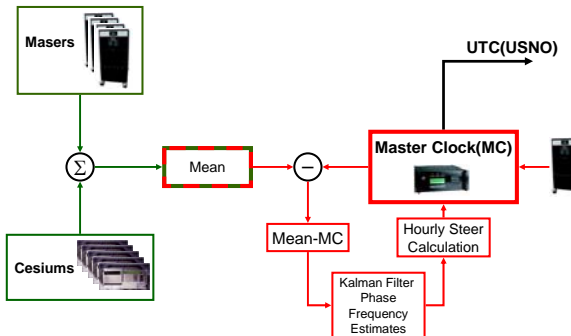


Figure 2. Present design block diagram.

The state-space model for a frequency standard steered by discrete frequency steps is given as:

$$\mathbf{X}_{t+\tau} = \Phi \mathbf{X}_t + \mathbf{B} u_t, \quad (1)$$

where $\mathbf{X} = \begin{bmatrix} x \\ y \end{bmatrix} = \begin{bmatrix} \text{phase offset} \\ \text{frequency offset} \end{bmatrix}$, $\Phi = \begin{bmatrix} 1 & \tau \\ 0 & 1 \end{bmatrix}$, $u_t = -\mathbf{G} \mathbf{X}_t = -[g_x \ g_y] \begin{bmatrix} x \\ y \end{bmatrix}$, and $\mathbf{B} = \begin{bmatrix} \tau \\ 1 \end{bmatrix}$.

Given the gain function G, the state-space equation can be written as:

$$\begin{bmatrix} x \\ y \end{bmatrix}_{t+\tau} = \begin{bmatrix} 1 - g_x \tau & (1 - g_y) \tau \\ -g_x & 1 - g_y \end{bmatrix} \begin{bmatrix} x \\ y \end{bmatrix}_t. \quad (2)$$

Figure 4 compares the controls of the daily steers of the previous system to the hourly steers of the present system. As expected, the hourly steers created a smoother response in the short term. The experimental setup used a common hydrogen maser with two separate frequency synthesizers and is shown in Figure 3.

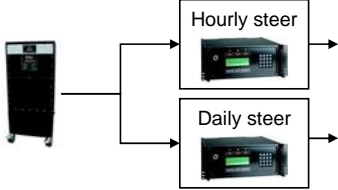


Figure 3. Common maser reference signal.

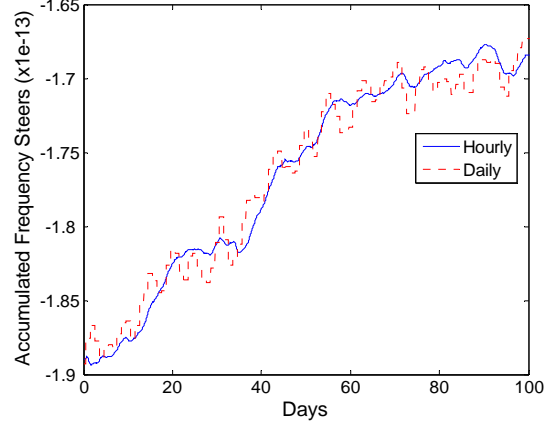


Figure 4. Comparison of accumulated frequencies from hourly and daily steering.

Actual performance of the present setup versus the real-time reference and a cesium mean are shown in Figure 5. The small (~ 1 ns) phase steps characteristic of the postprocessed model changes can be seen in the data. The MC steers are given in Figure 6 and are dominated by values within a band of $\pm 10^{-16}$.

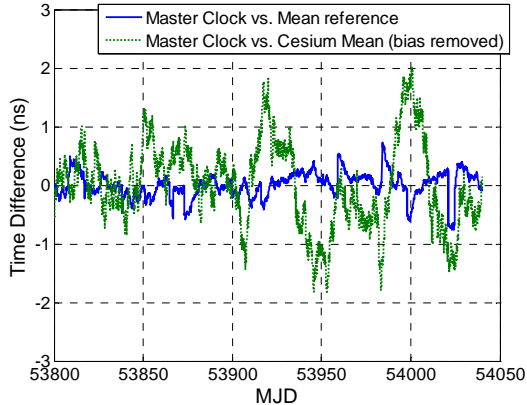


Figure 5. Time difference data.

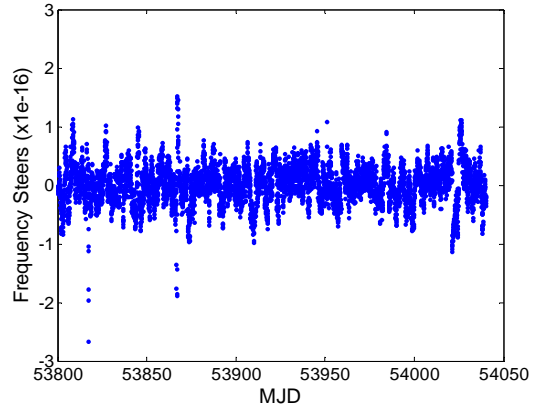


Figure 6. Master Clock steers.

FUTURE SYSTEM DESIGN

We are testing a design with separate means from the respective collections of hydrogen masers and cesiums [5]. The maser mean (MM) is steered to the cesium mean (CM) with a time constant of several weeks (see Figure 7). The steered MM preserves the short-term stability of the maser mean and gains the long-term performance of the CM. Like the previously described systems, the physical output is created by steering a hydrogen maser-based signal. In this design, models are used to remove initial characteristic rates and drifts from a maser when it is first introduced into the MM. The control design of the MM to CM is then expected to remove any nominal clock divergence from the initial model that would normally create a postprocessed recharacterization of the clock in the dynamic mean. Large changes in model or significant performance degradation result in the maser being removed from the mean. The smoother real-time MM allows for a tighter, more robust, control design for the physical output. The MM is created with data from a recently upgraded measurement system that is approximately an order of magnitude quieter than the measurement system used in the dynamic mean calculations and previous experiments [5].

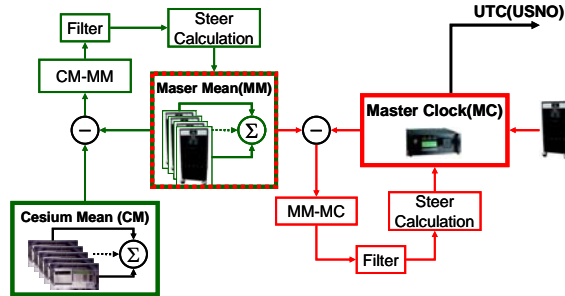


Figure 7. Future system block diagram.

The state-space model for the system described in Figure 7 is:

$$\mathbf{X}_{t+\tau} = \Phi \mathbf{X}_t + \mathbf{B} u_t$$

$$\mathbf{X} = \begin{bmatrix} x_{MM-AOG06} \\ y_{MM-AOG06} \\ x_{CM-MM} \\ y_{CM-MM} \end{bmatrix}, \quad \Phi = \begin{bmatrix} 1 & \tau & 0 & 0 \\ 0 & 1 & 0 & 0 \\ 0 & 0 & 1 & \tau \\ 0 & 0 & 0 & 1 \end{bmatrix}, \text{ and } \mathbf{B} = \begin{bmatrix} \tau & -\tau \\ 1 & -1 \\ 0 & \tau \\ 0 & 1 \end{bmatrix} \quad (3)$$

where x is phase difference, y is frequency difference, the control $u_t = -\mathbf{G}\mathbf{X}_t$, and \mathbf{G} is the control gain. The above equation can be rewritten as $\mathbf{X}_{t+\tau} = (\Phi - \mathbf{B}\mathbf{G})\mathbf{X}_t$.

Figure 8 shows the performance of the frequency synthesizer AOG06 versus the MM reference and also the MM versus the CM (see Figure 10). The small disturbance in the MM-AOG06 data near 53960 was caused by an issue with the environmental chamber that housed the reference maser. The Allan deviations of AOG06 and its reference maser are shown in Figure 9. The plot shows that the control has effectively removed the drift of the maser. There were 17 maser recharacterizations and weight changes over this period in the dynamic timescale compared to two maser deweighting in the MM over the same interval. The new design is more robust and exhibits excellent performance compared to the MC. This system is presently operating as a backup MC and is planned to transition to the primary MC after further evaluation.

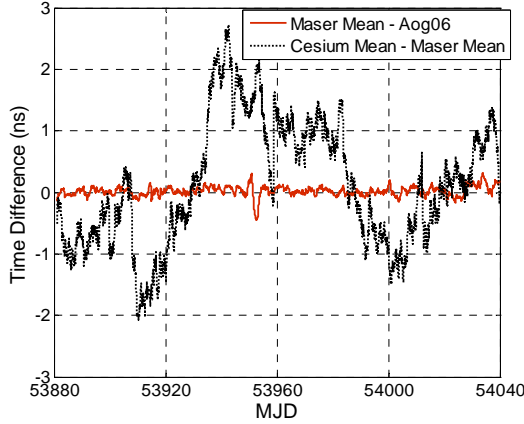


Figure 8. Measured time difference data.

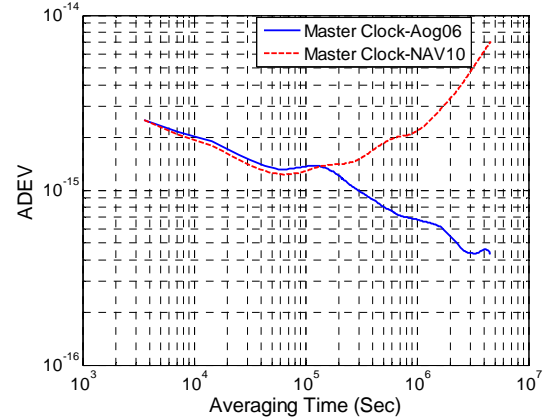


Figure 9. Stability comparison.

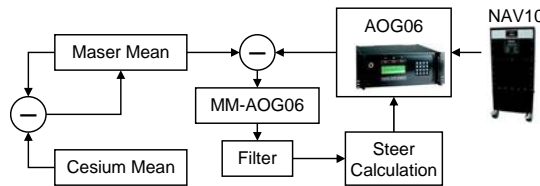


Figure 10. System setup for Figures 8 and 9.

STEERING TO UTC

One of the goals of the MC is to represent a high-quality real-time physical realization of UTC (the postprocessed international paper timescale defined by the BIPM). A block diagram describing how the MC is steered to UTC, using the month of December as an example, is shown in Figure 11.

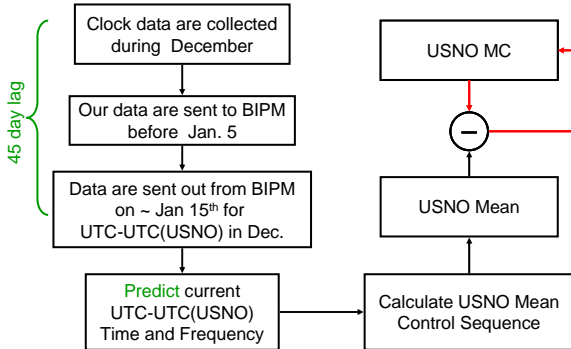


Figure 11. Example of control sequence calculation for December data.

Data from the BIPM are published monthly with a time lag ranging from approximately 15 to 45 days. Present time and frequency offsets are predicted from the given data, and then the sequence of frequency steers minimizing the control effort is determined.

The goal is to minimize the control effort, or so-called control energy,

$$\frac{1}{2} \sum_{k=0}^{N-1} u^2(k) \quad (4)$$

of the frequency steers $u(k)$ used to steer the MC to UTC [6,7]. The solution using the model given in (1) is

$$U = -\frac{6}{N(N+1)} \begin{bmatrix} \frac{1}{\tau} & \frac{2N-1}{3} \\ \frac{1}{\tau}(1-\frac{2}{N-1}) & -1+\frac{2N-1}{3} \\ \vdots & \vdots \\ -\frac{1}{\tau} & -(N-1)+\frac{2N-1}{3} \end{bmatrix} \begin{bmatrix} x(0) \\ y(0) \end{bmatrix} \text{ or,} \quad (5)$$

$$u(k) = \frac{6}{N(N+1)} \left[\left(1 - \frac{2k}{N-1}\right) \tau^{-1} x(0) + \left(\frac{2N-1}{3} - k\right) y(0) \right], \text{ for } k = 0 \dots N-1. \quad (6)$$

Figure 12 shows how the simulated control system using the above equation reacts to removing 3 ns of phase and 2×10^{-15} of frequency offsets with varying steering update intervals. As expected, the shorter intervals produced a smoother response.

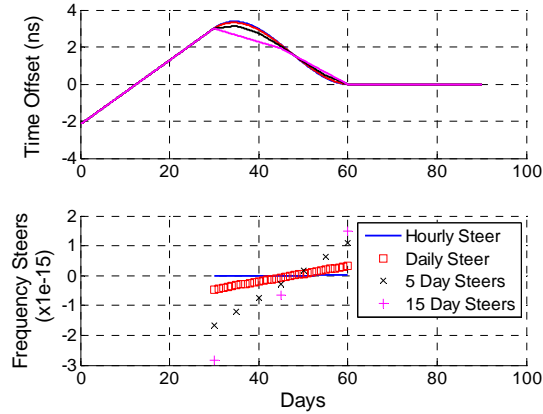


Figure 12. Response to removing 3 ns and 3×10^{-15} offsets.
(USNO).

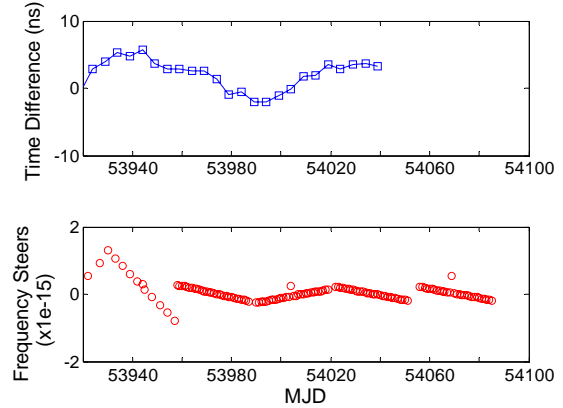


Figure 13. Top plot is UTC – UTC (USNO); bottom plot is the steers applied to UTC

Figure 13 shows the time difference between UTC and UTC (USNO) and the associated frequency steers. Prior to MJD 53960, steers were software-limited to an update rate of every 3 days; past that point, daily steers have been implemented. The outlying points on the plot are steers that match the TAI steers implemented by the BIPM.

CONCLUSION

Efforts are underway to improve both the robustness and performance of USNO Master Clock system. Designs are decreasing the time intervals between updates and tightening control parameters in both the internally derived systems and those referencing UTC. Performance tests verified the results that were predicted by simulations. Future work will include how to best incorporate atomic fountains into an appropriate reference timescale. We will also look into steering each maser independently to the CM and improving the predictors utilized in calculating the control sequences for steering to UTC.

ACKNOWLEDGMENT

The authors gratefully acknowledge the support provided by the Office of Naval Research (ONR) in the future system design work.

REFERENCES

- [1] L. A. Breakiron, 1992, “*Timescale algorithms combining cesium clocks and hydrogen masers*,” in Proceedings of the 23rd Annual Precise Time and Time Interval (PTTI) Applications and Planning Meeting, 3-5 December 1991, Pasadena, California (NASA CP-3159), pp.297-305.
- [2] D. Matsakis, M. Miranian, and P. Koppang, 1999, “*Steering the U.S. Naval Observatory (USNO) Master Clock*,” in Proceedings of the 1999 National Technical Meeting of the Institute of Navigation, 25-27 January 1999, San Diego, California, USA (ION, Alexandria, Virginia), pp. 871-880.
- [3] R. Brown and P. Hwang, 1992, **Introduction to Random Signals and Applied Kalman Filtering** (second edition, John Wiley & Sons, New York).
- [4] J. Skinner and P. Koppang, 2002, “*Effects of parameter estimation and control limits on steered frequency standards*,” in Proceedings of the 33rd Annual Precise Time and Time Interval (PTTI) Systems and Applications Meeting, 27-29 November 2001, Long Beach, California, USA (U.S. Naval Observatory, Washington, D.C.), pp. 399-405.
- [5] P. Koppang, D. Johns, and J. Skinner, 2004, “*Application of control theory in the formation of a timescale*,” in Proceedings of the 35th Annual Precise Time and Time Interval (PTTI) Systems and Applications Meeting, 2-4 December 2003, San Diego, California, USA (U.S. Naval Observatory, Washington, D.C.), pp. 319-326.
- [6] K. Ogata, 1995, **Discrete-Time Control Systems** (second edition, Prentice Hall, Englewood Cliffs, New Jersey).
- [7] P. Koppang and D. Matsakis, 2000, “*New steering strategies for the USNO Master Clock*,” in Proceedings of the 31st Annual Precise Time and Time Interval (PTTI) Systems and Applications Meeting, 7-9 December 1999, Dana Point, California, USA (U.S. Naval Observatory, Washington, D.C.), pp. 277-283.